PRAMEF2-mediated dynamic regulation of YAP signaling promotes tumorigenesis

Madhurima Ghosh[a] and Sanjeev Das[a,1]

[a]Molecular Oncology Laboratory, National Institute of Immunology, New Delhi 110067, India

Edited by Michael R. Green, University of Massachusetts Medical School, Worcester, MA, and approved August 25, 2021 (received for review March 22, 2021)

PRAMEF2 is a member of the PRAME multigene family of cancer testis antigens, which serve as prognostic markers for several cancers. However, molecular mechanisms underlying its role in tumorigenesis remain poorly understood. Here, we report that *PRAMEF2* is repressed under conditions of altered metabolic homeostasis in a FOXP3-dependent manner. We further demonstrate that PRAMEF2 is a BC-box containing substrate recognition subunit of Cullin 2–based E3 ubiquitin ligase complex. PRAMEF2 mediates polyubiquitylation of LATS1 kinase of the Hippo/YAP pathway, leading to its proteasomal degradation. The site for ubiquitylation was mapped to the conserved Lys860 residue in LATS1. Furthermore, LATS1 degradation promotes enhanced nuclear accumulation of the transcriptional coactivator YAP, resulting in increased expression of proliferative and metastatic genes. Thus, PRAMEF2 promotes malignant phenotype in a YAP-dependent manner. Additionally, elevated PRAMEF2 levels correlate with increased nuclear accumulation of YAP in advanced grades of breast carcinoma. These findings highlight the pivotal role of PRAMEF2 in tumorigenesis and provide mechanistic insight into YAP regulation.

PRAMEF2 | YAP | ubiquitylation | tumorigenesis

PRAMEF2 (PRAME Family Member 2) is a cancer testis antigen that belongs to the unique PRAME multigene family. PRAME is highly abundant and serves as a prognostic marker for several cancers including melanoma (1), neuroblastoma (2), and serous ovarian adenocarcinoma (3). In breast cancer, PRAME levels are significantly correlated with enhanced distant metastases and reduced overall patient survival (4, 5). Using biochemical and genomics approaches, PRAME has been characterized as a BC-box containing substrate recognition subunit of Cullin 2–based E3 ubiquitin ligase complex (6). PRAMEF2 has robust homology and similar expression patterns as PRAME, the founding member of the PRAME multigene family. However, the molecular mechanisms underlying its role in tumorigenesis remain unexplored.

The transcriptional coactivator YAP (YES-associated protein) is the nuclear effector of the Hippo signaling pathway. Inactivation of the Hippo kinase cascade results in the nuclear accumulation of YAP (7). In the nucleus, YAP binds to the transcription factor TEAD (TEA domain containing transcription factor) thereby regulating the expression of genes involved in diverse cellular processes including cellular proliferation, apoptosis, and metastasis (8). Thus, aberrant nuclear accumulation of YAP has been reported to be associated with several human malignancies (9).

In the present study, we report that *PRAMEF2* levels are down-regulated upon metabolic stress in a FOXP3-dependent manner. Using a proteomics approach, we further characterized PRAMEF2 as the substrate recognition subunit of Cullin 2–based E3 ligase complex. PRAMEF2 mediates LATS1 polyubiquitylation leading to its proteasomal degradation. Consequently, LATS1-mediated YAP phosphorylation is abrogated leading to its nuclear accumulation and induction of proliferative and metastatic genes. Thus, PRAMEF2 promotes tumorigenesis in a YAP-dependent manner.

Results

***PRAMEF2* Is Repressed by FOXP3 upon Metabolic Stress.** Cancer testis antigens have been reported to confer survival advantage to cancer cells under conditions of altered metabolic homeostasis (10). However, molecular insights into regulation of cancer testis antigens under such conditions remain unexplored. Hence, we examined the PRAMEF2 levels under metabolic stress conditions including glucose starvation, serum starvation, and metformin treatment. We observed that there was a significant decrease in the PRAMEF2 protein levels upon metabolic stress (Fig. 1*A*). We also observed a similar reduction in transcript levels, suggesting that PRAMEF2 was transcriptionally regulated (Fig. 1*B*). To delineate the mechanism of PRAMEF2 repression upon metabolic stress, we examined *PRAMEF2* promoter sequence for potential transcription factor binding sites. Our analysis revealed a FOXP3 binding site at −1.179 Kb position (Fig. 1*C*). FOXP3 is a member of the Forkhead family of transcription factors and has been reported to repress oncogenes including *Skp2* and *HER2*/*ERBB2* (11, 12). To investigate the role of FOXP3 in *PRAMEF2* repression, we examined the *PRAMEF2* levels upon metabolic stress, in the presence or absence of FOXP3. We observed that upon metabolic stress PRAMEF2 levels were down-regulated concomitant to increase in the FOXP3 levels (Fig. 1*D* and *SI Appendix*, Fig. S1 *A–C*). The decline in PRAMEF2 levels under metabolic stress conditions was abrogated upon FOXP3 depletion. Similar results were obtained in other cell types including ZR-751 and Human Mammary Epithelial Cells (HMECs) (*SI Appendix*, Fig. S1 *D* and *E*). Moreover, in the presence of ectopically expressed FOXP3, there was a significant decline in *PRAMEF2* transcript levels independent of glucose starvation conditions (*SI Appendix*, Fig. S1 *F* and *G*). To further corroborate the role of FOXP3 in *PRAMEF2* transcriptional regulation, we performed reporter assays (Fig. 1*E*). We observed robust repression of the *PRAMEF2*

Significance

PRAMEF2 belongs to the PRAME multigene family of cancer testis antigens, which serve as biomarkers for several cancers. However, its role in tumorigenesis remains unexplored. Here, we delineate PRAMEF2 regulation under low-nutrient conditions. We also show that it promotes proteasomal degradation of LATS1 kinase of the Hippo/YAP pathway. LATS1 down-regulation triggers nuclear accumulation of the transcriptional coactivator YAP, which induces the expression of proliferative and metastatic genes. Thus, PRAMEF2 promotes malignant phenotype in a YAP-dependent manner. Taken together, our findings reveal a pivotal role for PRAMEF2 in determining YAP oncogenic signaling, which has key implications for tumorigenesis.

Author contributions: M.G. and S.D. designed research; M.G. performed research; M.G. and S.D. contributed new reagents/analytic tools; M.G. and S.D. analyzed data; and M.G. and S.D. wrote the paper.

The authors declare no competing interest.

This article is a PNAS Direct Submission.

[1]To whom correspondence may be addressed. Email: sdas@nii.ac.in.

This article contains supporting information online at https://www.pnas.org/lookup/suppl/doi:10.1073/pnas.2105523118/-/DCSupplemental.

Published September 30, 2021.

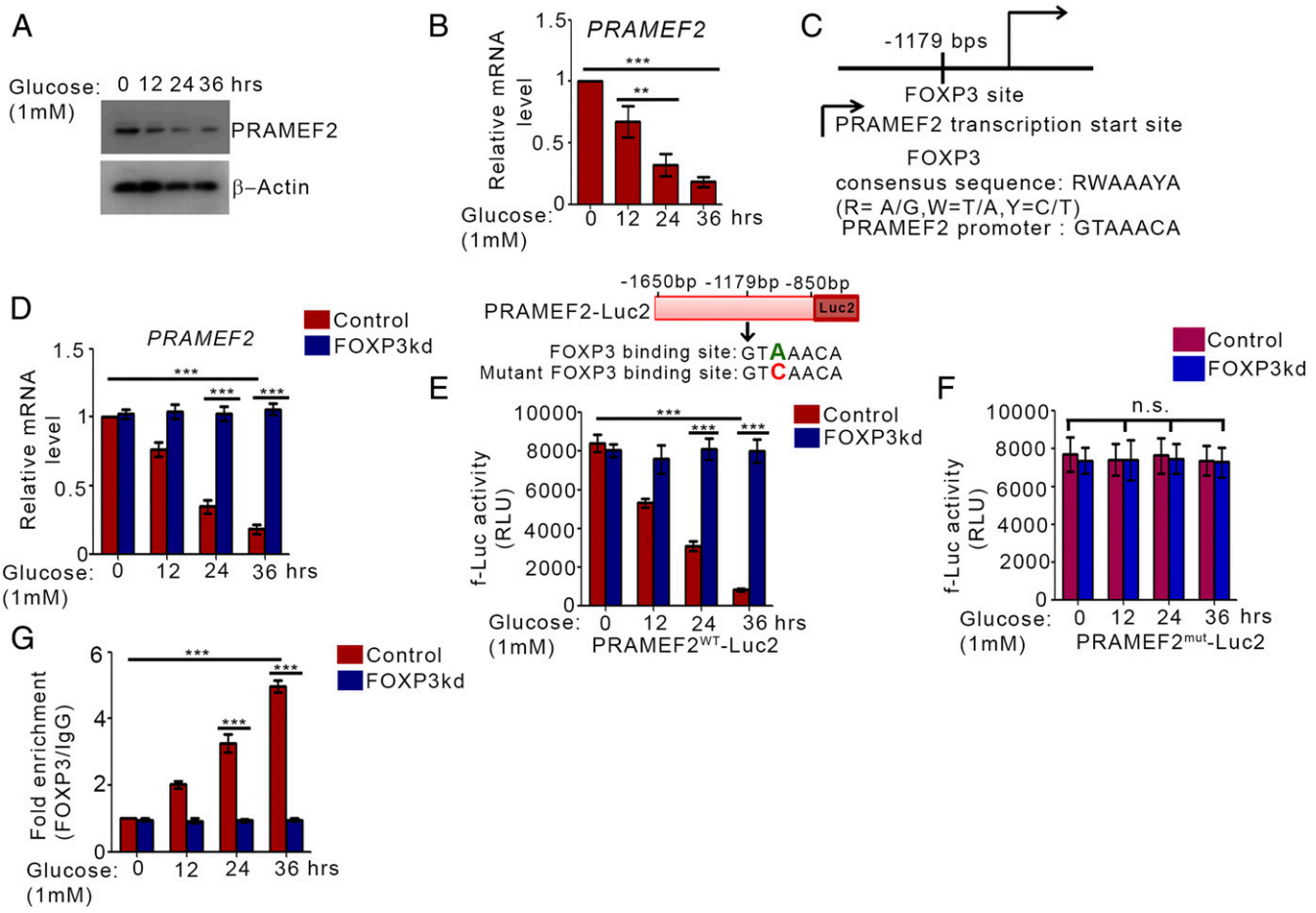

Fig. 1. *PRAMEF2* is transcriptionally repressed upon metabolic stress in a FOXP3-dependent manner. (*A*) MCF-7 cells were subjected to glucose starvation for the indicated time points. The cells were then harvested, and Western blotting was performed. (*B*) MCF-7 cells were subjected to glucose starvation for the indicated time points. RT-qPCR was then performed. Error bars are mean ± SD of three independent experiments with triplicate samples. ***$P < 0.0001$, **$P < 0.05$. (*C*) Schematic representation of the FOXP3 consensus binding site at the *PRAMEF2* promoter as indicated by the transcription factor database TRANSFAC. (*D*) MCF-7 cells were stably transfected (pooled zeomycin-resistant population) with control (scrambled) or FOXP3 short hairpin ribonucleic acid (shRNA). These cells were subjected to glucose starvation for the indicated time points. RT-qPCR was then performed. Error bars are mean ± SD of three independent experiments with triplicate samples. ***$P < 0.0001$, ***$P < 0.001$. (*E*) MCF-7 control (control) and FOXP3 knockdown (FOXP3kd) cells were transfected with the indicated luciferase reporter plasmid. At 24 h posttransfection, cells were subjected to glucose starvation for the indicated time points and luciferase reporter assay was then performed. ***$P < 0.0001$, ***$P < 0.001$. (*F*) MCF-7 control (control) and FOXP3 knockdown (FOXP3kd) cells were transfected with the indicated luciferase reporter plasmid. At 24 h posttransfection, cells were subjected to glucose starvation for the indicated time points and luciferase reporter assay was then performed. n.s., nonsignificant. (*G*) MCF-7 control (control) and FOXP3 knockdown (FOXP3kd) cells were subjected to glucose starvation for the indicated time points. ChIP assay was then performed with control IgG or FOXP3 antibody. Error bars are mean ± SD of three independent experiments with triplicate samples. ***$P < 0.0001$, ***$P < 0.001$.

promoter over the time course of metabolic stress, which was abrogated upon FOXP3 depletion. Moreover, when a reporter construct having mutant *PRAMEF2* promoter was used FOXP3-mediated repression was not observed (Fig. 1*F*). We next performed chromatin immunoprecipitation (ChIP) assay to examine the binding of FOXP3 to the *PRAMEF2* promoter. We detected increasing levels of FOXP3 at the *PRAMEF2* promoter upon metabolic stress, which was abolished upon FOXP3 depletion (Fig. 1*G*). Since previous studies suggest that repressive histone marks such as H3K9 trimethylation (H3K9me3) are associated with FOXP3 binding regions of the repressed genes (13), we performed sequential ChIP assays to examine the presence of such marks at *PRAMEF2* promoter. We observed an increase in H3K9 trimethylation at the *PRAMEF2* promoter upon metabolic stress, which was repressed upon FOXP3 depletion (*SI Appendix*, Fig. S1*H*). Since histone methyltransferase SUV39H1 has been reported to mediate H3K9 trimethylation, its presence at the *PRAMEF2* promoter was also investigated (14). An increased recruitment of SUV39H1 was detected at the *PRAMEF2* promoter over the time course of metabolic stress, which was abrogated upon FOXP3 depletion (*SI Appendix*, Fig. S1*I*). These results suggest that *PRAMEF2* is repressed upon metabolic stress in a FOXP3-dependent manner.

PRAMEF2, a BC-Box Protein, Is a Constituent of Cullin 2–Based E3 Ubiquitin Ligase Complex. To gain mechanistic insights into the role of PRAMEF2 in tumorigenesis, we employed a proteomics approach to identify PRAMEF2 interacting proteins (Fig. 2*A*). Among the several interacting partners identified, Cullin 2, Elongin B, Elongin C, and Rbx1 were of particular interest since PRAME has been reported to be a subunit of Cullin 2–based E3 ligases (6). In order to bind Elongin C, BC-box proteins contain a conserved sequence motif known as the BC-box, along with a downstream sequence called Cul-2 box that determines binding to Cullin-2 (15). Pairwise sequence alignment of PRAMEF2 with PRAME revealed the presence of these motifs at the N terminus of PRAMEF2 (Fig. 2*B*). To explore further, we performed gel filtration chromatography assay (Fig. 2*C*). We observed that Cullin 2, Elongin B, Elongin C, and Rbx1 eluted in the same

A

	Protein Symbol	Score Sequest HT	%Coverage	Unique Peptides
Ad-GFP	DDX1	48.19	19	4
	HSPA8	42.57	13	3
	NCL	35.90	16	1
	EZR	27.88	21	2
	LMNA	26.32	11	5
	EIF3L	29.14	27	1
	RUVBL2	21.07	16	3
	PSMC6	17.21	22	1
	SEPTIN7	14.36	9	2
	PHB2	11.89	7	5
Ad-PRAMEF2-HA-FLAG	FUBP2	171.23	52	23
	ELOB	**559.1**	**65**	**37**
	ELOC	**614.53**	**69**	**33**
	PRAMEF2	**697.81**	**87**	**44**
	RBX1	**419.80**	**71**	**31**
	CUL2	**509.42**	**76**	**42**
	LATS1	**356.04**	**60**	**29**
	WDR5	184.62	55	21
	FBX2	133.14	40	18
	DNAJB1	122.28	51	31
	YB1	112.31	52	14
	API5	132.09	47	22
	PTB	98.77	33	14
	DEK	108.01	37	20
	SNF5	94.50	26	10
	ANXA1	119.11	44	13

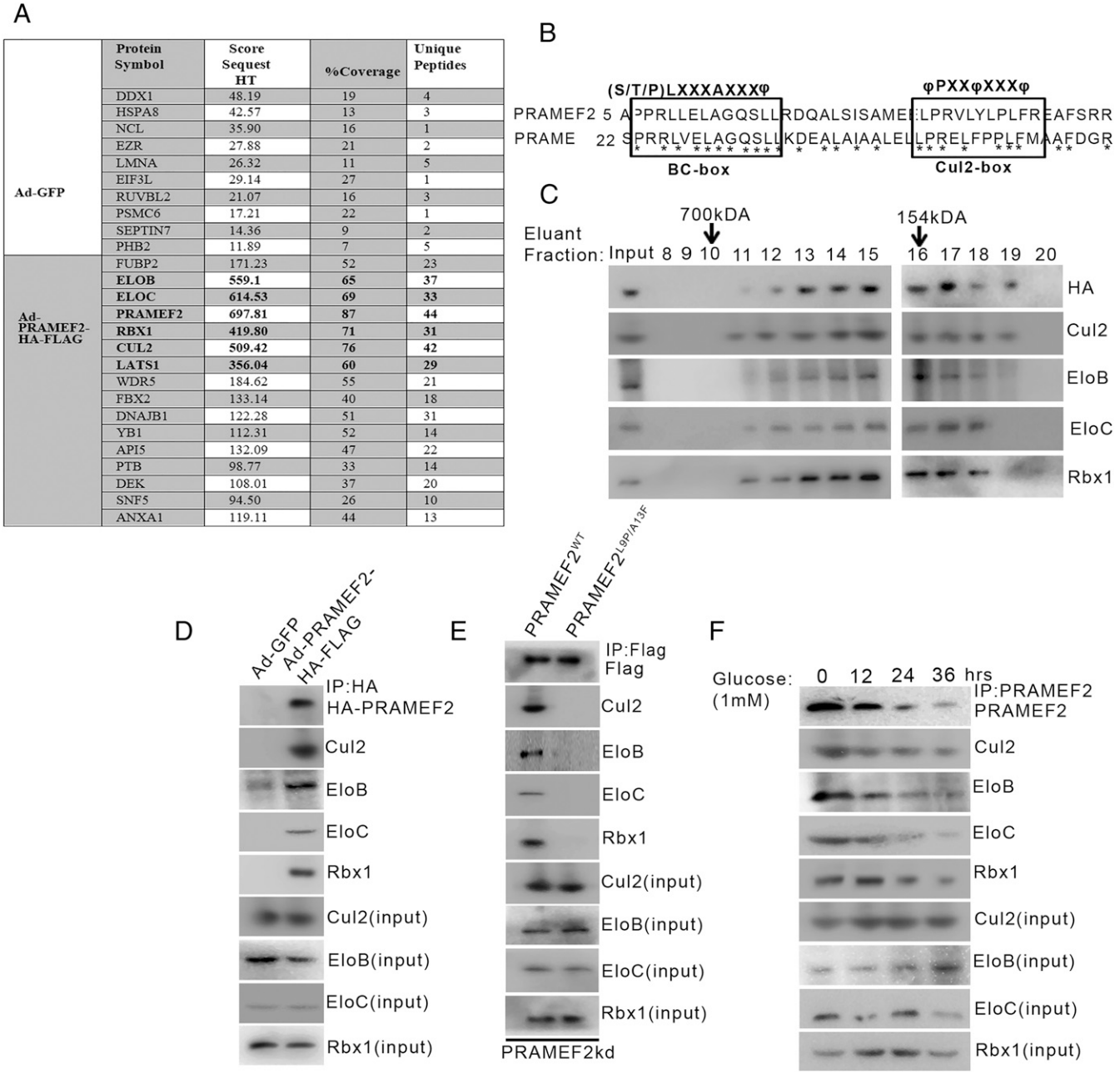

Fig. 2. PRAMEF2 is a part of Cullin 2–based E3 ligase complex. (*A*) MCF-7 cells were infected with adenovirus expressing GFP (Ad-GFP) or adenovirus expressing PRAMEF2 tagged with HA and FLAG epitopes (Ad-PRAMEF2 HF) for 24 h. The PRAMEF2-associated proteins were identified by immunoprecipitation followed by LC-MS/MS analysis. (*B*) Schematic representation of the BC-box and Cul2-box sequences at the N-terminal end of PRAMEF2 and PRAME proteins. (*C*) MCF-7 cells were infected with adenovirus expressing PRAMEF2 tagged with HA and FLAG epitopes (Ad-PRAMEF2 HF). At 24 h postinfection, cell extracts were subjected to size exclusion chromatography, followed by Western blotting. The numbers represent eluent fractions. (*D*) MCF-7 cells were infected with the indicated adenoviruses for 24 h. The cells were then harvested and subjected to immunoprecipitation using anti-HA antibody followed by Western blotting. (*E*) MCF-7 PRAMEF2 knockdown (PRAMEF2kd) cells were transfected with Flag-tagged wild-type PRAMEF2 ($PRAMEF2^{WT}$) or BC-box mutant PRAMEF2 ($PRAMEF2^{L9P/A13F}$) constructs. At 24 h posttransfection, the cells were harvested and subjected to immunoprecipitation using anti-FLAG antibody followed by Western blotting. (*F*) MCF-7 cells were subjected to glucose starvation for the indicated time points. The cells were then harvested and subjected to immunoprecipitation using anti-PRAMEF2 antibody followed by Western blotting.

fractions as PRAMEF2 indicating that they could be part of a multisubunit complex. Moreover, these proteins coimmunoprecipitated with PRAMEF2, which was not observed in case of BC-box mutant PRAMEF2 ($PRAMEF2^{L9P/A13F}$) (Fig. 2 *D* and *E* and *SI Appendix*, Fig. S2*A*). Furthermore, concomitant to down-regulation of PRAMEF2 under metabolic stress conditions, the levels of coimmunoprecipitated Cul2, Elo B, Elo C, and Rbx1 also declined (Fig. 2*F*). Taken together, these results suggest that PRAMEF2 is a component of a Cullin 2–based E3 ligase complex, which is down-regulated upon metabolic stress.

PRAMEF2 Mediates LATS1 Ubiquitylation and Targets It for Proteasomal Degradation. In our proteomic screen, we also identified LATS1 as a PRAMEF2 interacting protein. LATS1 is a Ser/Thr Kinase that functions as a tumor suppressor by regulating cell proliferation and apoptosis (16, 17). However, little is

known about its role under conditions of altered metabolic homeostasis. Thus, we examined the interaction between PRAMEF2 and LATS1 under metabolic stress conditions. Our results indicated that the interaction between LATS1 and PRAMEF2 is down-regulated over the time course of metabolic stress (Fig. 3 *A* and *B* and *SI Appendix*, Fig. S2 *B–E*). Furthermore, there was an increase in the LATS1 protein levels concomitant to the decline in PRAMEF2 levels upon metabolic stress while there was no significant change in transcript levels of *LATS1* (Fig. 3 *C* and *D* and *SI Appendix*, Fig. S2 *F* and *G*). Similar observations were made in other cell types (*SI Appendix*, Fig. S2 *H–M*). To further examine whether PRAMEF2 had any effect on the half-life of LATS1 protein, we performed a cycloheximide chase assay (*SI Appendix*, Fig. S3*A*). Our results suggest that there is a significant PRAMEF2-dependent decline in LATS1 protein levels in the presence of cycloheximide, with a distinct reduction in half-life.

Since protein stability is frequently regulated by the ubiquitin-proteasome degradation pathway, we investigated the effects of the proteasome inhibitor MG-132 on LATS1 levels. Upon MG-132 treatment, LATS1 levels were constitutively elevated over the time course of metabolic stress with no significant change in the transcript levels (Fig. 3*E*). As our earlier results suggest that PRAMEF2 is a component of a Cullin 2–based E3 ligase complex, we examined LATS1 levels under metabolic stress conditions, in the presence or absence of PRAMEF2. LATS1 levels were up-regulated upon glucose starvation, concomitant to the decline in PRAMEF2 levels. However, LATS1 levels were constitutively elevated under starvation conditions in the absence of PRAMEF2 (Fig. 3*F*). We next determined whether PRAMEF2 mediates LATS1 ubiquitylation. We observed that LATS1 is polyubiquitylated under unstressed conditions, which is down-regulated upon metabolic stress, concomitant to the decline in PRAMEF2 levels. In the absence of PRAMEF2 or in the presence of BC-box mutant PRAMEF2 ($PRAMEF2^{L9P/A13F}$), LATS1 polyubiquitylation was abrogated (Fig. 3*G* and *SI Appendix*, Fig. S3 *B–D*). Similar results were obtained in other cell types (*SI Appendix*, Fig. S3 *E* and *F*). We further observed that LATS1 polyubiquitylation was K48 linked (Fig. 3*H*). Moreover, LATS1 polyubiquitylation was abrogated in the presence of mutant ubiquitin (K48R) (*SI Appendix*, Fig. S3*G*).

In order to map the site of PRAMEF2-mediated LATS1 polyubiquitylation, we performed GST-pulldown assays under conditions of glucose starvation. The GST-LATS1 fusion protein comprising the amino acids 843 to 1,130 was polyubiquitylated under unstressed conditions, which was abrogated upon metabolic stress (Fig. 3*I*). The specific region of polyubiquitylation was further narrowed down to GST-LATS1 fusion protein comprising amino acids 843 to 942 (Fig. 3*J*). To identify the specific site of polyubiquitylation, we mutated each of the three lysine residues in this region. We observed that the mutation of K860 residue specifically disrupted K48-linked LATS1 polyubiquitylation even though the interaction could still be observed (Fig. 3*K* and *SI Appendix*, Fig. S3 *H–J*). Similar results were obtained in other cell types (*SI Appendix*, Fig. S3 *K* and *L*). Furthermore, protein sequence analysis of the LATS1 region encompassing amino acids 848 to 876 suggests that the K860 site is conserved across diverse organisms (*SI Appendix*, Fig. S4*A*). Taken together, these results indicate that PRAMEF2 mediates K48-linked polyubiquitylation of LATS1 at K860 resulting in its proteasomal degradation, which is disrupted upon metabolic stress.

PRAMEF2 Promotes YAP Nuclear Translocation. LATS1 is known to phosphorylate YAP resulting in its cytoplasmic retention (18, 19). Hence, we next sought to investigate the effect of PRAMEF2 on YAP phosphorylation. We observed that the levels of phosphorylated YAP were up-regulated, concomitant to the increase in LATS1 levels and the decline in PRAMEF2 levels upon glucose starvation (Fig. 4*A*). However, upon depletion of PRAMEF2 phosphorylated YAP levels were constitutively elevated over the starvation period, which was abrogated upon depletion of LATS1 or codepletion of PRAMEF2 and LATS1. Moreover, in the presence of ubiquitylation-resistant LATS1 mutant ($LATS1^{K860R}$) or BC-box mutant PRAMEF2 ($PRAMEF2^{L9P/A13F}$) YAP was constitutively phosphorylated (Fig. 4 *B* and *C* and *SI Appendix*, Fig. S4 *B* and *C*). Similar results were obtained in other cell types (*SI Appendix*, Fig. S4 *D* and *E*). These results suggest that PRAMEF2 determines YAP phosphorylation status.

We next investigated the effect of PRAMEF2 on YAP cellular localization under metabolic stress conditions. Our results indicate that under unstressed conditions, YAP is present in the nucleus while upon metabolic stress it was phosphorylated and retained in the cytoplasm (Fig. 4*D*). However, in the absence of PRAMEF2, YAP was constitutively phosphorylated and present in cytoplasm. Previous reports suggest that 14-3-3 binds to phosphorylated YAP resulting in its cytoplasmic retention, while dephosphorylated YAP interacts with the transcription factor TEAD in the nucleus (18, 20). Our results suggest that YAP interacted with 14-3-3 upon metabolic stress, while in the presence of ubiquitylation-resistant LATS1 mutant ($LATS1^{K860R}$) the interaction was observed irrespective of stress conditions (Fig. 4*E*). On the other hand, YAP interacted with TEAD only under unstressed conditions, while in the presence of LATS1 mutant ($LATS1^{K860R}$) no interaction was detected. Thus, our data indicate that PRAMEF2-mediated LATS1 polyubiquitylation results in abrogation of YAP phosphorylation, which promotes its nuclear translocation.

PRAMEF2 Induces Proliferative and Metastatic Genes in a YAP-Dependent Manner. YAP is a transcriptional coactivator that has been reported to promote the expression of genes involved in various processes driving breast tumorigenesis including proliferation, invasion, and metastasis (21). Hence, in order to study the effect of PRAMEF2 on YAP-mediated transactivation, we examined the levels of genes reported to be associated with breast tumorigenesis (22). Our results indicate that several genes encompassing diverse pathways were down-regulated upon metabolic stress concomitant with the decline in PRAMEF2 levels. Moreover, upon PRAMEF2 depletion the levels of these genes were constitutively down-regulated (Fig. 5*A*). To gain additional mechanistic insights, we codepleted LATS1 along with PRAMEF2 and examined the transcript levels of key genes involved in various cancer-associated pathways including cell proliferation, apoptosis, and metastasis (Fig. 5*B* and *SI Appendix*, Fig. S5 *A* and *B*). We observed that upon depletion of LATS1 or codepletion of PRAMEF2 and LATS1, *CCNA2*, *TWIST1*, *SNAI2*, *BIRC2*, and *CDK6* were constitutively up-regulated. Similar observations were made in the presence of phospho-dead YAP mutant (YAP^{S127A}) and upon PRAMEF2 depletion in the presence of phospho-dead YAP mutant (YAP^{S127A}). Concurring results were also obtained in other cell types (*SI Appendix*, Fig. S5 *C* and *D*). To further delineate the mechanism, we performed ChIP assay to examine the recruitment of YAP at the promoter of these genes (Fig. 5*C*). We observed a decline in the levels of YAP detected at the promoter of these genes upon metabolic stress, which was further down-regulated in the absence of PRAMEF2. However, upon depletion of LATS1 or codepletion of PRAMEF2 and LATS1 robust recruitment at the promoters was observed irrespective of stress conditions, as was the case in the presence of YAP^{S127A} and upon PRAMEF2 depletion in the presence of YAP^{S127A}. Taken together, our results suggest that PRAMEF2-promoted nuclear localization of YAP results in induction of genes involved in key cancer-associated pathways.

PRAMEF2-Mediated YAP Nuclear Translocation Is Critical for Its Oncogenic Functions. We next investigated the effect of PRAMEF2-mediated YAP activation on malignant phenotype. We observed that depletion of PRAMEF2 resulted in significant reduction of

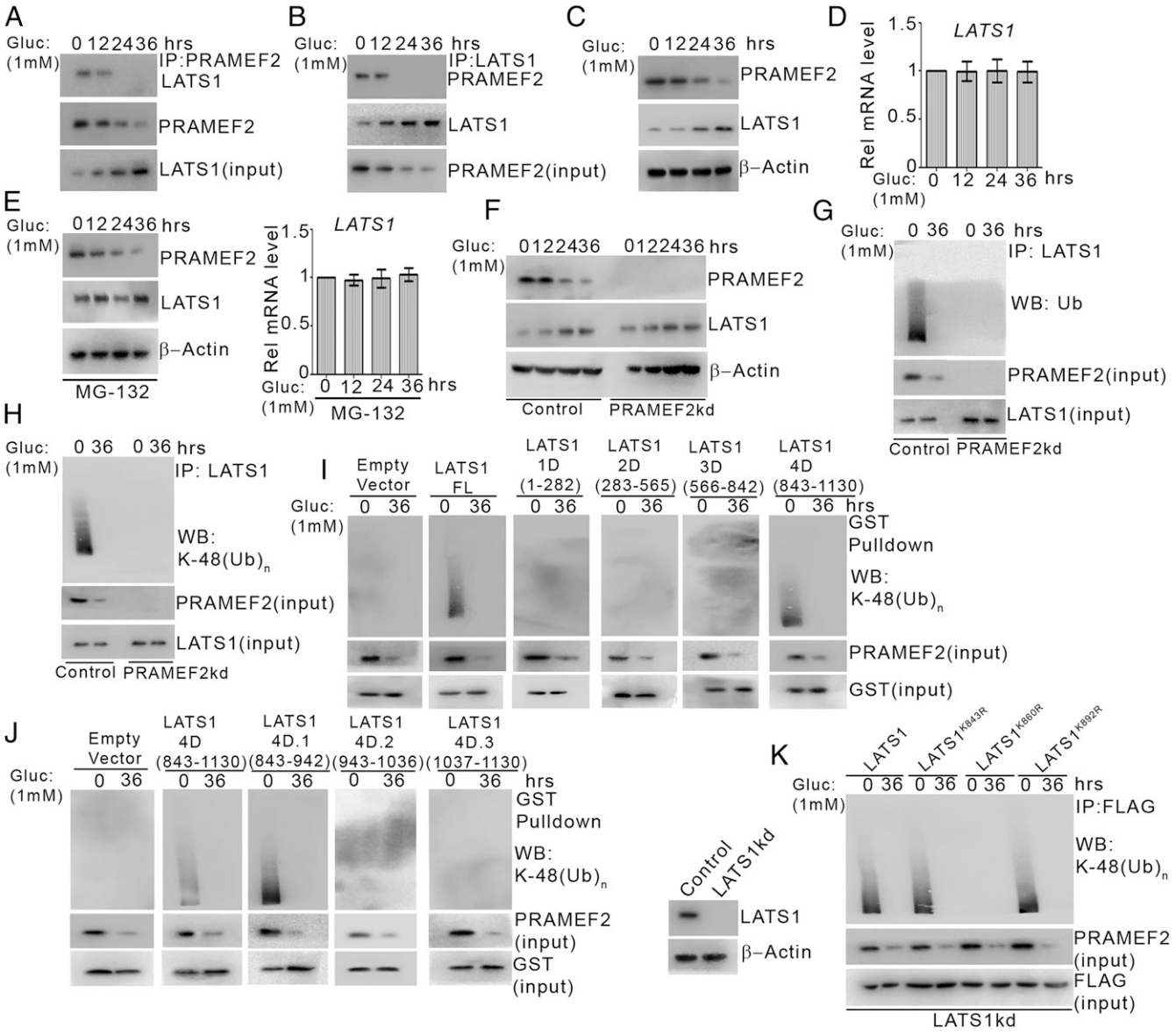

Fig. 3. LATS1 is ubiquitylated in a PRAMEF2-dependent manner. (*A*) MCF-7 cells were subjected to glucose starvation for the indicated time points. The cells were then harvested and subjected to immunoprecipitation using anti-PRAMEF2 antibody followed by Western blotting. (*B*) MCF-7 cells were subjected to glucose starvation for the indicated time points. The cells were then harvested and subjected to immunoprecipitation using anti-LATS1 antibody followed by Western blotting. (*C*) MCF-7 cells were subjected to glucose starvation for the indicated time points. The cells were then harvested, and Western blotting was performed. (*D*) MCF-7 cells were subjected to glucose starvation for the indicated time points. RT-qPCR was then performed. Error bars are mean ± SD of three independent experiments with triplicate samples. (*E*) MCF-7 cells were subjected to glucose starvation for the indicated time points and treated with MG132 for the last 6 h of the starvation period. (*Left*) The cells were then harvested, and Western blotting was performed. (*Right*) RT-qPCR was performed. Error bars are mean ± SD of three independent experiments with triplicate samples. (*F*) MCF-7 control (control) and PRAMEF2 knockdown (PRAMEF2kd) cells were subjected to glucose starvation for the indicated time points. The cells were then harvested, and Western blotting was performed. (*G*) MCF-7 control (control) and PRAMEF2 knockdown (PRAMEF2kd) cells were subjected to glucose starvation for the indicated time points and treated with MG132 (10 μM) for the last 6 h of the starvation period. Cells were then harvested and subjected to immunoprecipitation using anti-LATS1 antibody followed by Western blotting. (*H*) MCF-7 control (control) and PRAMEF2 knockdown (PRAMEF2kd) cells were subjected to glucose starvation for the indicated time points and treated with MG132 (10 μM) for the last 6 h of the starvation period. Cells were then harvested and subjected to immunoprecipitation using anti-LATS1 antibody followed by Western blotting. (*I*) MCF-7 cells were transfected with constructs expressing full-length (FL) or different domains of LATS1 (1D: 1 to 282 amino acids [aa], 2D: 283 to 565 aa, 3D: 566 to 842 aa, 4D: 843 to 1130 aa) as GST fusion proteins. At 24 h posttransfection, the cells were subjected to glucose starvation for the indicated time points and treated with MG132 (10 μM) for the last 6 h of starvation period. Cell lysates were then prepared and subjected to GST pull-down followed by Western blotting. (*J*) MCF-7 cells were transfected with constructs expressing different subdomains of LATS1 (4D: 843 to 1130 aa, 4D.1: 843 to 942 aa, 4D.2: 943 to 1036 aa, 4D.3: 1037 to 1130 aa) as GST fusion proteins. At 24 h posttransfection, the cells were subjected to glucose starvation for the indicated time points and treated with MG132 (10 μM) for the last 6 h of starvation period. Cell lysates were then prepared and subjected to GST pull down followed by Western blotting. (*K*) MCF-7 cells were stably transfected (pooled zeomycin-resistant population) with control (scrambled) or LATS1 shRNA. (*Left*) MCF-7 control (control) and LATS1 knockdown (LATS1kd) cells were harvested, and Western blotting was performed. (*Right*) MCF-7 LATS1 knockdown cells were transfected with FLAG-tagged wild-type LATS1, $LATS1^{K843R}$, $LATS1^{K860R}$, or $LATS1^{K892R}$. At 24 h posttransfection, the cells were subjected to glucose starvation for the indicated time points and treated with MG132 (10 μM) for the last 6 h of starvation period. Cells were then harvested and subjected to immunoprecipitation using anti-FLAG antibody followed by immunoblotting.

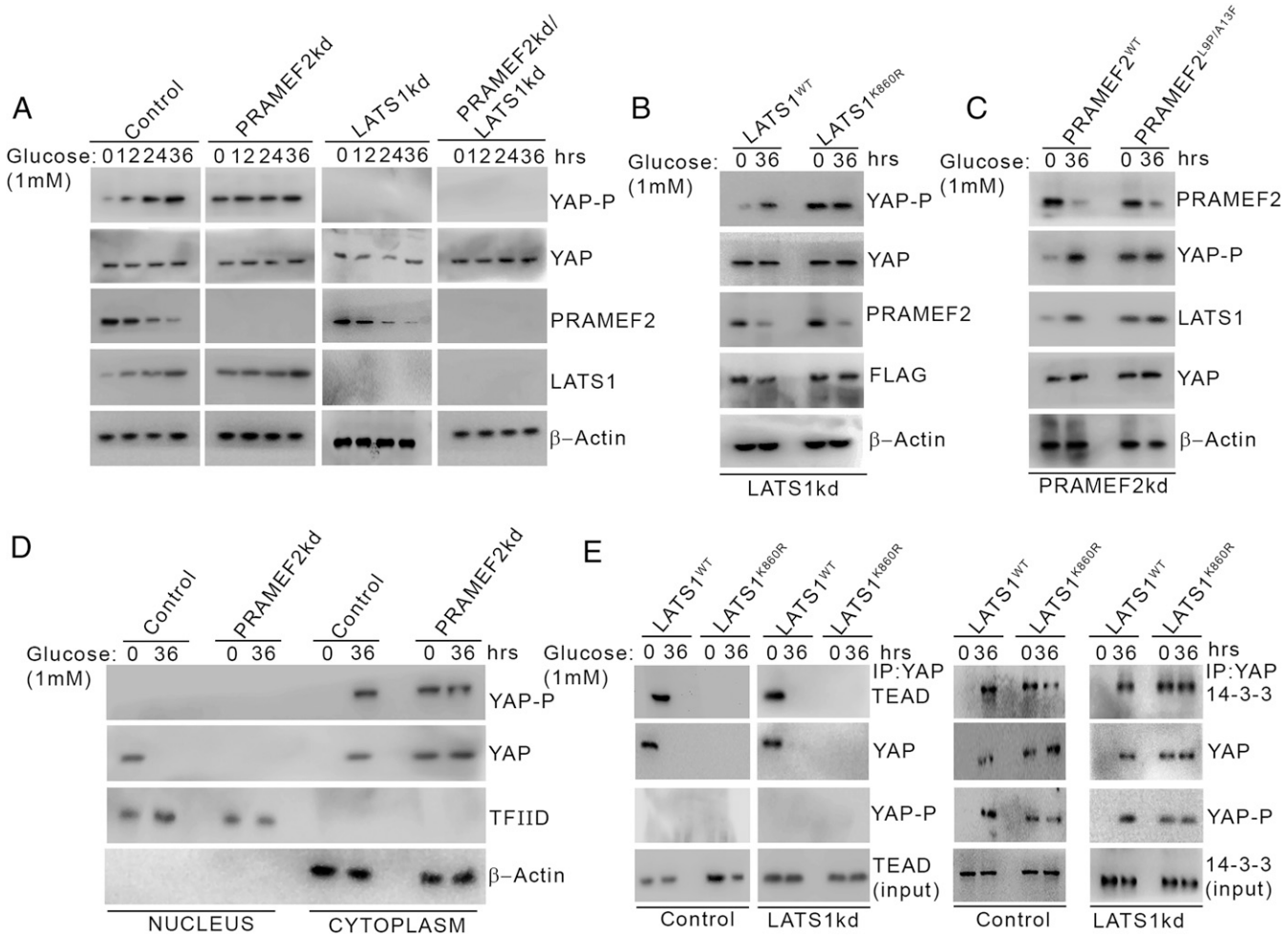

Fig. 4. PRAMEF2 inhibits LATS1-mediated YAP phosphorylation. (*A*) MCF-7 control (control), PRAMEF2 knockdown (PRAMEF2kd), LATS1 knockdown (LATS1kd), and PRAMEF2/LATS1 double knockdown (PRAMEF2kd/LATS1kd) cells were subjected to glucose starvation for the indicated time points. The cells were then harvested, and Western blotting was performed. (*B*) MCF7 LATS1 knockdown (LATS1kd) cells were transfected with FLAG-tagged wild-type LATS1 and LATS1^{K860R} constructs. At 24 h posttransfection, the cells were subjected to glucose starvation for the indicated time points. The cells were then harvested, and Western blotting was performed. (*C*) MCF-7 PRAMEF2 knockdown (PRAMEF2kd) cells were transfected with Flag-tagged wild-type PRAMEF2 (PRAMEF2^{WT}) or BC-box mutant PRAMEF2 (PRAMEF2$^{L9P/A13F}$) constructs. At 24 h posttransfection, the cells were subjected to glucose starvation for the indicated time points. The cells were then harvested, and Western blotting was performed. (*D*) MCF-7 control (control) and PRAMEF2 knockdown (PRAMEF2kd) cells were subjected to glucose starvation for the indicated time points. The cells were then harvested, and Western blotting was performed from the cytoplasmic and nuclear fractions. (*E*) MCF-7 control (control) and LATS1 knockdown (LATS1kd) cells were transfected with FLAG-tagged wild-type LATS1 and LATS1^{K860R} constructs. At 24 h posttransfection, the cells were subjected to glucose starvation for the indicated time points. (*Left*) Nuclear extracts were prepared and subjected to immunoprecipitation using anti-YAP antibody followed by Western blotting. (*Right*) Cytoplasmic extracts were prepared and subjected to immunoprecipitation using anti-YAP antibody followed by Western blotting.

proliferation capacity (Fig. 6*A*). However, depletion of LATS1 or codepletion of PRAMEF2 and LATS1, which promotes constitutive nuclear localization of YAP, resulted in enhanced proliferative capacity. Additionally, presence of YAP^{S127A} and PRAMEF2 depletion in the presence of YAP^{S127A} also augmented the proliferative capacity even in the absence of PRAMEF2. We then examined the effect of PRAMEF2–YAP axis on invasiveness and migration potential under conditions of altered metabolic homeostasis. Our results indicated that under metabolic stress conditions invasiveness and migration potential were down-regulated. Additionally, depletion of PRAMEF2 resulted in reduced invasiveness and migration potential irrespective of stress conditions (Fig. 6 *B* and *C* and *SI Appendix*, Fig. S6 *A* and *B*). However, invasiveness and migration potential was up-regulated upon depletion of LATS1 or codepletion of PRAMEF2 and LATS1. Concurring observations were made in the presence ofYAP^{S127A} and upon PRAMEF2 depletion in the presence of YAP^{S127A}. Conversely, ectopic expression of ubiquitylation-resistant LATS1 mutant (LATS1^{K860R}) significantly down-regulated invasiveness and migration potential. Similar results were obtained in ZR-751 cells (*SI Appendix*, Fig. S6 *C* and *D*). We further examined the role of PRAMEF2-dependent YAP activation on anchorage independent growth (Fig. 6*D*). Our results indicated that anchorage independent growth was repressed under metabolic stress conditions. However, upon PRAMEF2 depletion, anchorage independent growth was constitutively down-regulated. Depletion of LATS1, codepletion of PRAMEF2 and LATS1, and ectopic expression of YAP^{S127A} or PRAMEF2 depletion in the presence of YAP^{S127A} promoted anchorage independent growth. These results suggest that PRAMEF2-mediated YAP activation is pivotal to its oncogenic potential.

PRAMEF2 Promotes Aggressive Tumor Phenotype in a YAP-Dependent Manner. We next examined the role of YAP in determining PRAMEF2-promoted tumor malignancy in an orthotopic breast

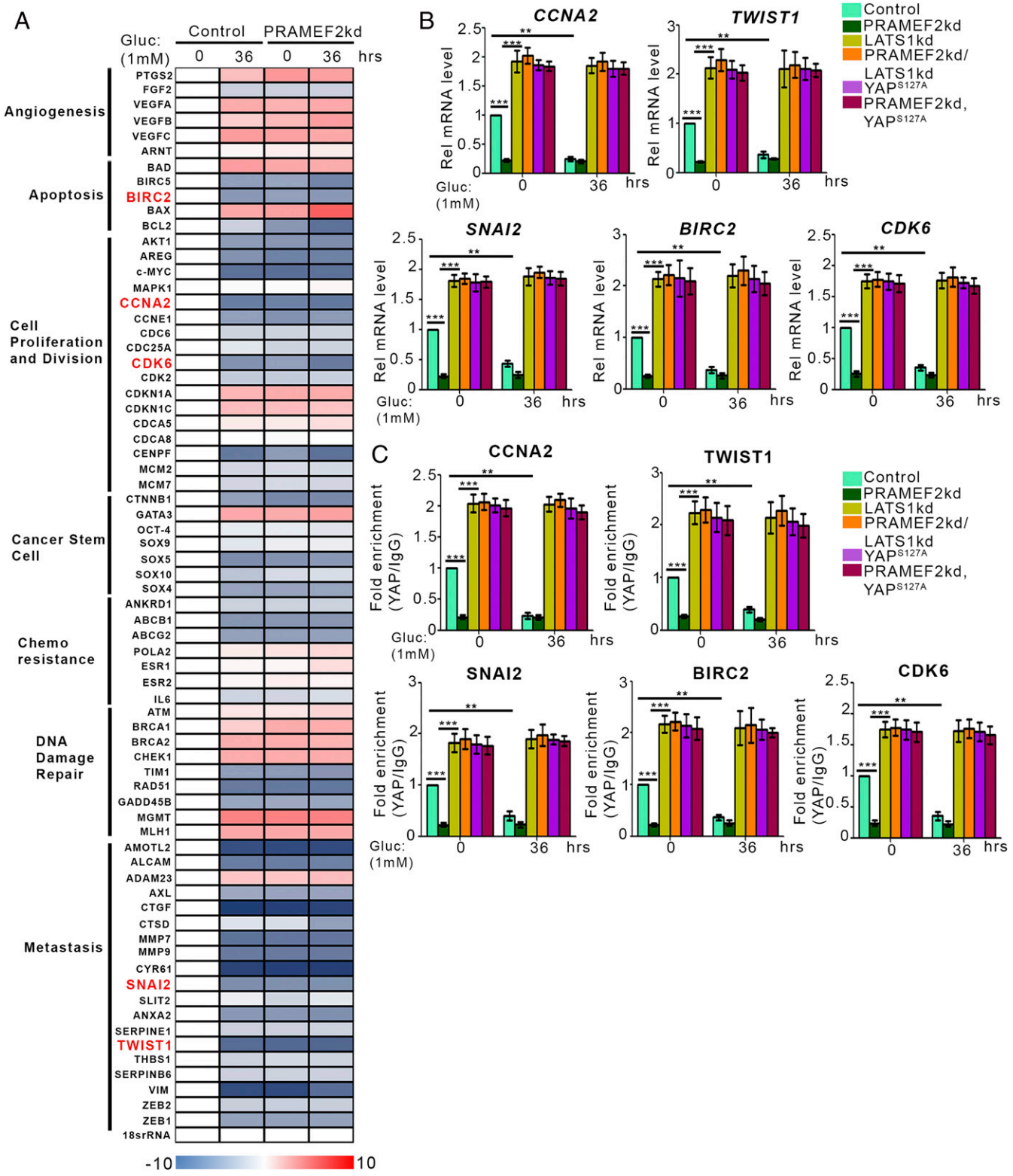

Fig. 5. PRAMEF2 promotes YAP transactivation function. (*A*) MCF-7 control (control) and PRAMEF2 knockdown (PRAMEF2kd) cells were subjected to glucose starvation for the indicated time points. Relative messenger ribonucleic acid (mRNA) levels were analyzed by RT-qPCR. Heat map comparing relative mRNA levels is shown. Blue and red indicate down-regulation or up-regulation, respectively. (*B*) MCF-7 control and PRAMEF2 knockdown cells were stably transfected with FLAG-tagged YAP^{S127A}. MCF-7 control (control), PRAMEF2 knockdown (PRAMEF2kd), LATS1 knockdown (LATS1kd), and PRAMEF2/LATS1 double knockdown (PRAMEF2kd/LATS1kd) cells as well as MCF-7 control and PRAMEF2 knockdown cells expressing YAP^{S127A} (YAP^{S127A} and PRAMEF2kd, YAP^{S127A}) were subjected to glucose starvation for the indicated time points. RT-qPCR was then performed. Error bars are mean ± SD of three independent experiments with triplicate samples. $^{**}P < 0.05$, $^{***}P < 0.001$. (*C*) MCF-7 control (control), PRAMEF2 knockdown (PRAMEF2kd), LATS1 knockdown (LATS1kd), and PRAMEF2/LATS1 double knockdown (PRAMEF2kd/LATS1kd) cells as well as MCF-7 control and PRAMEF2 knockdown cells expressing YAP^{S127A} (YAP^{S127A} and PRAMEF2kd, YAP^{S127A}) were subjected to glucose starvation for the indicated time points. ChIP assay was then performed with control IgG or YAP antibody. Error bars are mean ± SD of three independent experiments with triplicate samples. $^{**}P < 0.05$, $^{***}P < 0.001$.

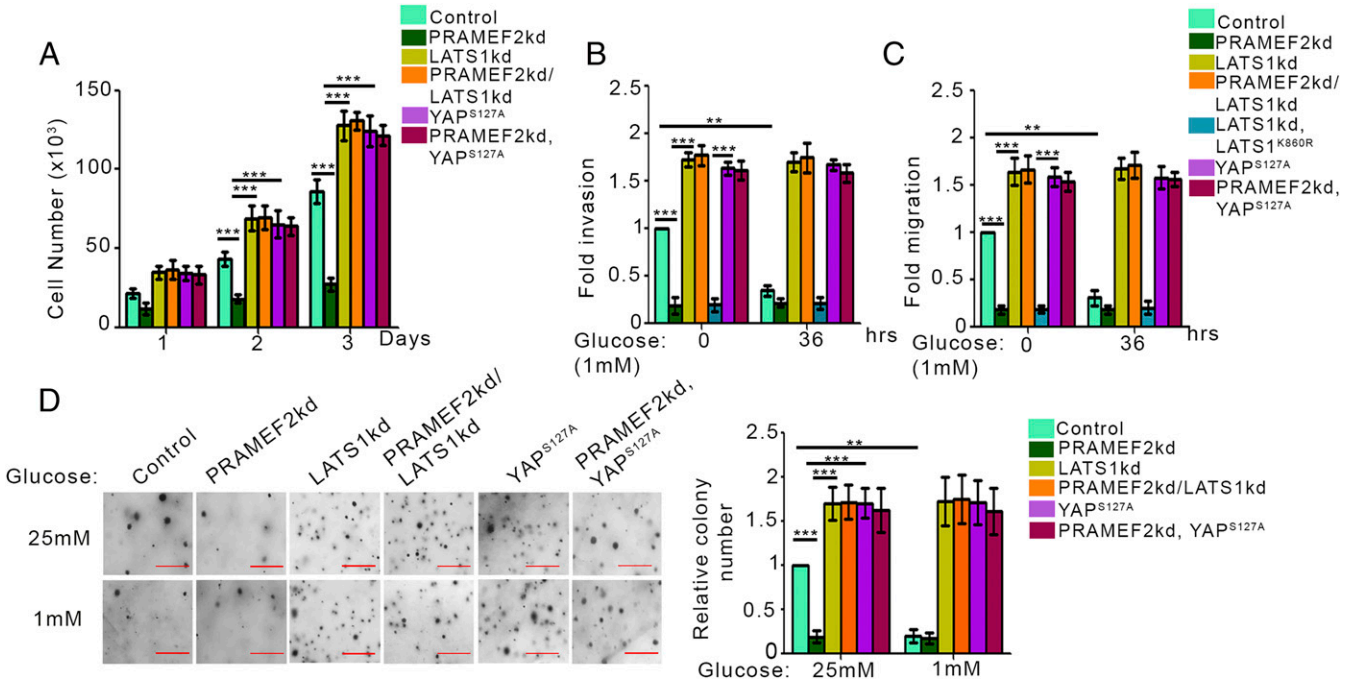

Fig. 6. YAP plays a key role in determining PRAMEF2 oncogenic functions. (*A*) MCF-7 control (control), PRAMEF2 knockdown (PRAMEF2kd), LATS1 knockdown (LATS1kd), and PRAMEF2/LATS1 double knockdown (PRAMEF2kd/LATS1kd) cells as well as MCF-7 control and PRAMEF2 knockdown cells expressing YAP^{S127A} (YAP^{S127A} and PRAMEF2kd, YAP^{S127A}) were cultured in complete medium and counted at the indicated time points. Error bars are means ± SD of three independent experiments with duplicate samples. ***$P < 0.001$. (*B*) MCF-7 control (control), PRAMEF2 knockdown (PRAMEF2kd), LATS1 knockdown (LATS1kd), PRAMEF2/LATS1 double knockdown (PRAMEF2kd/LATS1kd), and LATS1 knockdown cells expressing FLAG-tagged $LATS1^{K860R}$ mutant as well as MCF-7 control and PRAMEF2 knockdown cells expressing YAP^{S127A} (YAP^{S127A} and PRAMEF2kd, YAP^{S127A}) were subjected to glucose starvation for the indicated time points. In vitro invasion of cells was measured as the percentage of cells migrating to the bottom chamber. Error bars represent mean ± SD of three independent experiments with triplicate samples. **$P < 0.05$, ***$P < 0.001$. (*C*) MCF-7 control (control), PRAMEF2 knockdown (PRAMEF2kd), LATS1 knockdown (LATS1kd), PRAMEF2/LATS1 double knockdown (PRAMEF2kd/LATS1kd), and LATS1 knockdown cells expressing FLAG-tagged $LATS1^{K860R}$ mutant cells as well as MCF-7 control and PRAMEF2 knockdown cells expressing YAP^{S127A} (YAP^{S127A} and PRAMEF2kd, YAP^{S127A}) were subjected to glucose starvation for the indicated time points. The migration potential of cells was measured as the percentage of cells migrating to the bottom chamber. Error bars represent mean ± SD of three independent experiments with triplicate samples. **$P < 0.05$, ***$P < 0.001$. (*D*) MCF-7 control (control), PRAMEF2 knockdown (PRAMEF2kd), LATS1 knockdown (LATS1kd), and PRAMEF2/LATS1 double knockdown (PRAMEF2kd/LATS1kd) cells as well as MCF-7 control and PRAMEF2 knockdown cells expressing YAP^{S127A} (YAP^{S127A} and PRAMEF2kd, YAP^{S127A}) were seeded in soft agar and maintained in 25 mM or 1 mM glucose as indicated. (*Left*) Representative images of colonies in soft agar are shown. (Scale bars, 200 μm.) (*Right*) Numbers of colonies per well are represented as mean ± SD of three independent experiments. **$P < 0.05$, ***$P < 0.001$.

cancer model. Our results indicated that abrogation of PRAMEF2 expression resulted in significantly smaller tumors. However, depletion of LATS1, codepletion of PRAMEF2 and LATS1, and ectopic expression of YAP^{S127A} or PRAMEF2 depletion in the presence of YAP^{S127A} resulted in a significant increase in tumor size (Fig. 7 *A* and *B* and *SI Appendix*, Fig. S7 *A* and *B*). Furthermore, numerous metastatic nodules were detected in the liver and lungs (Fig. 7 *A*, *C*, and *D* and *SI Appendix*, Fig. S7 *A* and *C*). We also observed higher numbers of circulating tumor cells in these mice (*SI Appendix*, Fig. S7 *D* and *E*). This was further corroborated by the reduced levels of epithelial marker E-cadherin and up-regulation of mesenchymal markers vimentin and fibronectin observed in the primary tumors, which is indicative of predisposition of these tumors to metastasize (*SI Appendix*, Fig. S7*F*). Thus, we concluded that YAP is critical for PRAMEF2-mediated tumor growth and metastasis.

Several previous studies have reported the dysregulation of LATS1 and YAP to be associated with breast cancer (23). Hence, we next examined the levels of PRAMEF2, LATS1, phosphorylated YAP, and YAP in different grades of breast carcinoma (Fig. 7*E*). We observed that PRAMEF2 levels were higher in breast carcinoma as compared to normal adjacent tissue while the levels of LATS1 and Phosphorylated YAP were down-regulated. Moreover, with increasing aggressiveness of breast carcinoma, the levels of PRAMEF2 were up-regulated while there was a marked decline in the levels of LATS1 and phosphorylated YAP (Fig. 7 *F–H*). Furthermore, there was increased nuclear accumulation of YAP in advanced grades of breast carcinoma (*SI Appendix*, Fig. S7 *G* and *H*). Thus, our data suggest that the PRAMEF2 up-regulation and consequent enhanced nuclear localization of YAP is critical for breast tumor progression.

Discussion

Rapid proliferation as well as abnormal vasculature can create conditions of nutrient deprivation in the tumor microenvironment in diverse cancers including breast cancer (24). Nutrient insufficiency can activate growth inhibitory signaling pathways (25). On the other hand, oncogene activation can induce metabolic reprogramming to help cancer cells survive nutrient limitations and sustain uncontrolled proliferation. In our study, we report that PRAMEF2-mediates polyubiquitylation and subsequent proteasomal degradation of LATS1 to activate YAP oncogenic transcriptional program. However, under nutrient deprivation conditions PRAMEF2-promoted proliferative signaling is repressed. Thus, our findings provide mechanistic insights on the oncogenic role of PRAMEF2. It will be of interest to use proteomics-based approaches to identify other targets of PRAMEF2 involved in malignant transformation.

FOXP3, a member of the Forkhead/winged-helix (FKH) family of transcription factors, plays a major role in T cell development

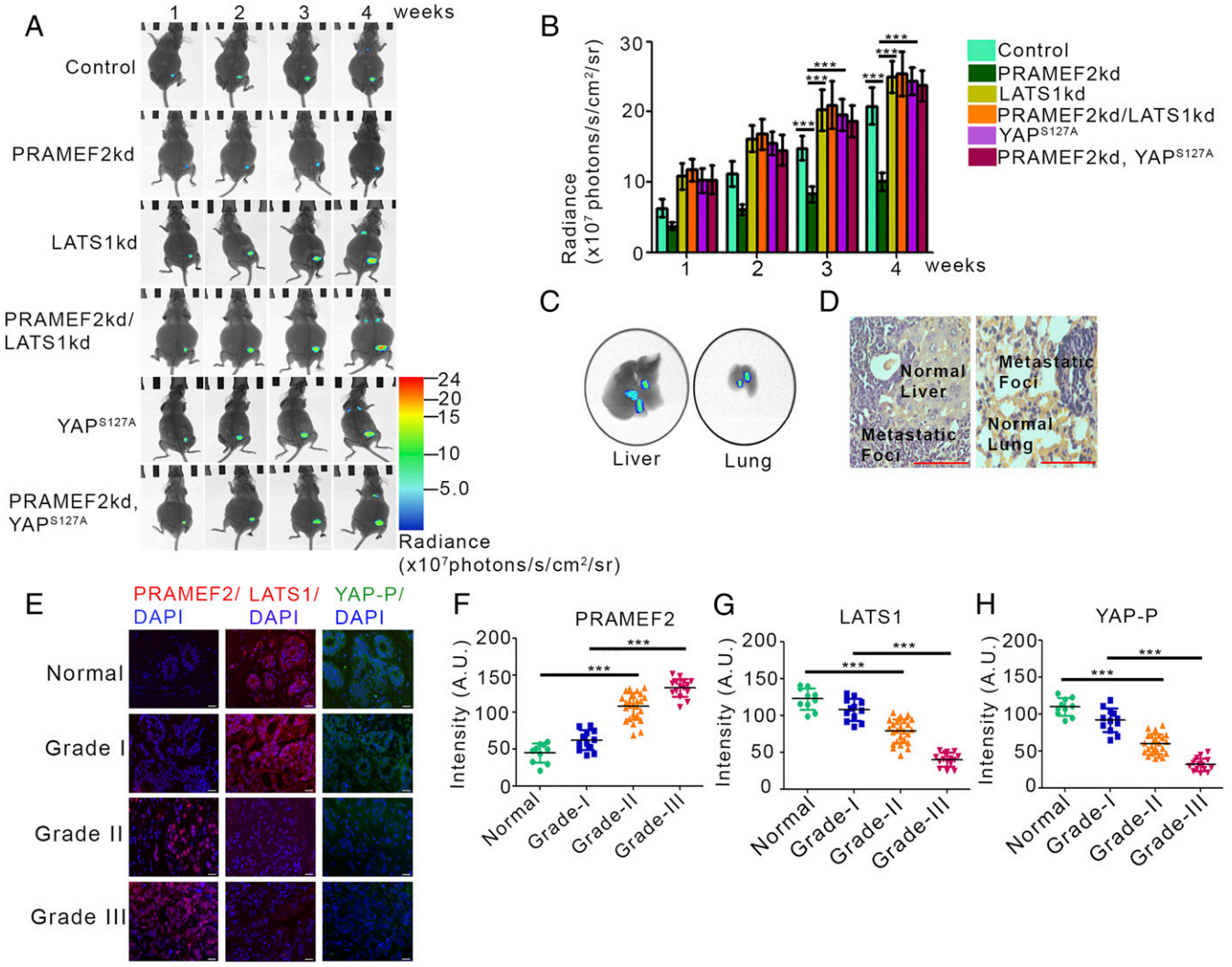

Fig. 7. YAP is critical for PRAMEF2-promoted aggressive tumor phenotype. (*A*) MCF-7^{Luc2} cells were stably transfected (pooled zeomycin-resistant population) with control (scrambled), PRAMEF2, LATS1, or PRAMEF2 along with LATS1 shRNA as indicated. MCF-7^{Luc2} and PRAMEF2 knockdown cells were stably transfected with Flag-tagged YAP^{S127A} (pooled G418-resistant population). These cells were orthotopically injected into the mammary fat pad of nude mice. Bioluminescence imaging was performed weekly. Representative images are shown. The data shown are representative of three independent experiments using five individual mice per group. (*B*) Bioluminescence quantification (*A, Above*) was performed at indicated time points. The data shown are representative of three independent experiments using five individual mice per group. Error bars are mean ± SD from five individual mice ($n = 5$ mice per group). ***$P < 0.001$. (*C* and *D*) At the end of 4 wk, organs from mice orthotopically implanted with MCF-7^{Luc2} PRAMEF2/LATS1 knockdown cells in *A* (*Above*) were harvested and examined by ex vivo imaging (*C*) as well as hematoxylin and eosin staining (*D*) to examine metastases. Representative images are shown. The data shown are representative of three independent experiments using five individual mice per group. (Scale bar, 50 μm.) (*E*) Representative images of immunostaining of PRAMEF2, LATS1, and phosphorylated-YAP on sections of normal breast tissue and different grades of human breast carcinoma. DAPI was used to counterstain nuclei. (Scale bar, 20 μm.) (*F*) Quantification of PRAMEF2 levels in normal breast tissue and different grades of human breast carcinoma. The data shown are representative of three independent experiments. Error bars are mean ± SD, ***$P < 0.0001$. (*G*) Quantification of LATS1 levels in normal breast tissue and different grades of human breast carcinoma. The data shown are representative of three independent experiments. Error bars are mean ± SD, ***$P < 0.0001$. (*H*) Quantification of phosphorylated-YAP levels in normal breast tissue and different grades of human breast carcinoma. The data shown are representative of three independent experiments. Error bars are mean ± SD, ***$P < 0.0001$.

and activity (26). It has also been reported to function as a tumor suppressor in breast and prostate cancer. It represses *HER-2/ErbB2* and *Skp2* expression to inhibit cell proliferation. Thus, widespread deletion and somatic mutations of FOXP3 are observed in breast cancer (12). In the case of prostate cancer, it represses *MYC* oncogene to induce growth arrest (27). Our studies suggest that FOXP3 represses *PRAMEF2* under conditions of altered metabolic homeostasis to down-regulate the oncogenic YAP signaling. Thus, our findings provide additional insights into the diverse pathways regulated by FOXP3.

LATS1 is a Ser/Thr Kinase that plays a pivotal role in the Hippo/YAP signaling pathway. It integrates several upstream signals to regulate the activity of its substrate YAP through phosphorylation-dependent cytoplasmic sequestration (18). Consistent with its role as a tumor suppressor, LATS1 has been reported to be down-regulated in several human cancers (28–30). But the molecular mechanisms underlying LATS1 regulation are poorly understood. Using exogenous overexpression-based studies, Itch, WWP1, and NEDD4 E3 ligases have been reported to ubiquitylate LATS1 and target it for proteasomal degradation (31–33). However, the pertinence of these ubiquitylation events in LATS1 regulation under physiological conditions is yet unclear. Our studies delineate the role of PRAMEF2 in the regulation of LATS1 under metabolic stress conditions.

PRAMEF2 mediates LATS1 polyubiquitylation at the conserved K860 residue leading to its proteasomal degradation. Upon metabolic stress, PRAMEF2 is down-regulated resulting in LATS1 stabilization. Thus, our findings reveal a pivotal role for PRAMEF2 in temporal regulation of LATS1 and hence YAP signaling, under conditions of altered metabolic homeostasis.

In the canonical Hippo/YAP Pathway, YAP is a transcriptional coactivator that binds to the transcription factor TEAD in the nucleus (20) and modulates the expression of genes involved in cell proliferation, apoptosis, metastasis, and other cancer-related pathways (34). YAP mediates transactivation of several genes implicated in cell proliferation including *Ki67, c-myc*, and *SOX4*. Furthermore, the expression of several negative regulators of apoptosis such as *BIRC5*/*Survivin* and *BIRC2*/*cIAP1* are also induced robustly in a YAP-dependent manner. Thus, dysregulation of YAP has been linked to hepatocellular carcinoma (7). YAP has also been reported to induce the expression of *TWIST1*, which promotes metastasis in clear cell renal carcinoma (35). In breast cancers, YAP has been reported to form a transactivation complex with ZEB1 resulting in the increased expression of several target genes implicated in epithelial–mesenchymal transition including *ANKRD1, CYR61*, and *CTGF* (36). Even though the dependency scores (DepMap) from genome-wide CRISPR-knockout screens for *PRAMEF2*, *LATS1*, and *YAP* do not exhibit significant correlation (37), our data suggests that PRAMEF2 promotes malignant phenotype in a YAP-dependent manner. PRAMEF2-mediated LATS1 degradation induces nuclear translocation of YAP, which triggers the expression of proliferative and metastatic genes. However, FOXP3-mediated *PRAMEF2* repression under low-nutrient conditions attenuates YAP oncogenic signaling. In conclusion, our findings highlight the complexity of mechanisms by which Hippo/YAP signaling can be regulated. Furthermore, our data highlight a key role for PRAMEF2 in determining tumorigenesis.

Methods

Cell Lines and Culture Conditions. MCF-7 cells were cultured in Dulbecco's modified Eagle medium (DMEM) containing 10% fetal bovine serum (FBS) (Invitrogen), 100 U/mL penicillin, and 100 μg/mL streptomycin at 37 °C. ZR-751 cells were cultured in Roswell Park Memorial Institute (RPMI)-1640 containing FBS, 100 U/mL penicillin, and 100 μg/mL streptomycin at 37 °C. HMECs were cultured in serum-free mammary epithelial cell growth medium-containing supplements, growth factors, bovine pituitary extracts, 50 U/mL penicillin, and 50 μg/mL streptomycin at 37 °C. The cell lines were obtained from American Type Culture Collection, authenticated, and routinely checked for mycoplasma contamination. Recombinant adenoviruses were amplified, and titration was performed as previously reported (38). Cells were grown to ∼50 to 70% confluency followed by infection with recombinant adenovirus at a multiplicity of infection of 10 to 20. Adenovirus expressing GFP (Ad-GFP) was used as a negative control. To induce glucose starvation, cells were grown to ∼50% confluency and were then cultured in glucose-free DMEM (Invitrogen) and RPMI-1640 (Invitrogen) containing dialyzed FBS (Invitrogen) and 1 mM glucose (Sigma-Aldrich). Reagents including metformin and MG132 were purchased from Sigma-Aldrich.

Transfection and Luciferase Assay. Transfections were carried out using Lipofectamine 3000 (Invitrogen) for MCF-7 cells and ZR-751 cells and Lipofectamine 2000 (Invitrogen) for HMECs following the manufacturer's instructions. Briefly, cells were allowed to reach 70% confluency at the time of transfection. Lipid–DNA complexes were prepared by adding DNA and Lipofectamine to serum-free medium and incubated at room temperature for 30 min. The cells were washed and the Lipid–DNA complexes were added. The amount of plasmid DNA was kept constant with empty vector in transient transfection experiments. After 6 h, the media volume was doubled with serum-free DMEM and supplemented with serum to attain a final concentration of 10% serum.

For luciferase assays, human *PRAMEF2* promoter fragment (−1,650 to −850) was cloned into the pGL4.24 vector (Promega) to obtain PRAMEF2-luc reporter construct. The PRAMEF2^{mut}-luc2 reporter construct was generated by site-directed mutagenesis (Mutagenex). The cells were harvested 24 h posttransfection, and luciferase activity was determined using Dual Luciferase Reporter assay system (Promega) as per the manufacturer's protocol. Briefly, cell extracts were prepared in 1X Passive Lysis Buffer, supplied by the manufacturer. In total, 20 μl cell extracts were added to 100 μl Luciferase Assay Reagent II, and Firefly luciferase activity was measured with a luminometer (Berthold systems). This signal was quenched by addition of 100 μl Stop and Glo reagent, followed by measuring the Renilla luciferase activity. The difference in transfection efficiency across samples was normalized by cotransfecting pRL-TK, which expresses Renilla luciferase. Error bars are mean ± SD of three independent experiments with duplicate samples.

Sequential Immunoprecipitation and Liquid Chromatography with Tandem Mass Spectrometry. MCF-7 cells were infected with recombinant adenovirus expressing PRAMEF2 tagged with HA and FLAG epitopes. Ad-GFP was used as a negative control. At 24 h postinfection, whole-cell extracts were prepared. Preclearing of the cell lysates was done using normal rabbit IgG and Protein A agarose slurry by incubation on a rotating platform for 2 h, at 4 °C. The cell extracts were then immunoprecipitated with anti-FLAG antibody-conjugated agarose beads (Santa Cruz) by incubating overnight on a rotor, at 4 °C. The beads were washed three times, and elution was performed by incubating the beads with 3X FLAG peptide (Sigma) for 30 min on ice. This elution was repeated twice, and the eluent fractions were pooled for a subsequent round of immunoprecipitation using anti-HA antibody-conjugated agarose beads (Santa Cruz). Washing and elution with HA peptide (Sigma-Aldrich) was performed in the same conditions as with 3X FLAG peptide. The final eluate thus obtained was resolved on a 7% sodium dodecyl sulphate-polyacrylamide gel electrophoresis, and protein bands were visualized by silver staining. The bands were excised and analyzed by reverse-phase LC-MS/MS (ITSI Biosciences). The MS data were processed using the tandem mass spectrometry data analysis program Sequest HT.

Soft Agar Assay. The soft agar assay was performed as described previously (39). Briefly, 2.5×10^3 cells were suspended in 1.5 mL medium containing 0.4% agar and overlaid on 1% agar in 6-well culture plates. The plates were incubated for 3 wk, and DMEM was added intermittently. After 3 wk, staining was performed with Nitroblue Tetrazolium chloride (Sigma). Images were captured using an inverted microscope (Nikon) and colonies were enumerated.

Data Availability. All study data are included in the article and/or *SI Appendix*.

ACKNOWLEDGMENTS. We thank the members of the Molecular Oncology Laboratory for helpful discussions. We also acknowledge the financial support from National Institute of Immunology Core Fund.

1. C. Haqq *et al*., The gene expression signatures of melanoma progression. *Proc. Natl. Acad. Sci. U.S.A.* **102**, 6092–6097 (2005).
2. A. Oberthuer, B. Hero, R. Spitz, F. Berthold, M. Fischer, The tumor-associated antigen PRAME is universally expressed in high-stage neuroblastoma and associated with poor outcome. *Clin. Cancer Res.* **10**, 4307–4313 (2004).
3. K. Partheen *et al*., Four potential biomarkers as prognostic factors in stage III serous ovarian adenocarcinomas. *Int. J. Cancer* **123**, 2130–2137 (2008).
4. P. Doolan *et al*., Prevalence and prognostic and predictive relevance of PRAME in breast cancer. *Breast Cancer Res. Treat.* **109**, 359–365 (2008).
5. M. T. Epping, A. A. Hart, A. M. Glas, O. Krijgsman, R. Bernards, PRAME expression and clinical outcome of breast cancer. *Br. J. Cancer* **99**, 398–403 (2008).
6. A. Costessi *et al*., The tumour antigen PRAME is a subunit of a Cul2 ubiquitin ligase and associates with active NFY promoters. *EMBO J.* **30**, 3786–3798 (2011).
7. J. Dong *et al*., Elucidation of a universal size-control mechanism in Drosophila and mammals. *Cell* **130**, 1120–1133 (2007).
8. B. Zhao, L. Li, Q. Lei, K. L. Guan, The Hippo-YAP pathway in organ size control and tumorigenesis: An updated version. *Genes Dev.* **24**, 862–874 (2010).
9. A. A. Steinhardt *et al*., Expression of Yes-associated protein in common solid tumors. *Hum. Pathol.* **39**, 1582–1589 (2008).
10. R. R. Florke Gee *et al*., Emerging roles of the MAGE protein family in stress response pathways. *J. Biol. Chem.* **295**, 16121–16155 (2020).
11. T. Zuo *et al*., FOXP3 is a novel transcriptional repressor for the breast cancer oncogene SKP2. *J. Clin. Invest.* **117**, 3765–3773 (2007).
12. T. Zuo *et al*., FOXP3 is an X-linked breast cancer suppressor gene and an important repressor of the HER-2/ErbB2 oncogene. *Cell* **129**, 1275–1286 (2007).
13. F. Pan *et al*., Eos mediates Foxp3-dependent gene silencing in CD4+ regulatory T cells. *Science* **325**, 1142–1146 (2009).
14. S. Rea *et al*., Regulation of chromatin structure by site-specific histone H3 methyltransferases. *Nature* **406**, 593–599 (2000).
15. A. Kibel, O. Iliopoulos, J. A. DeCaprio, W. G. Kaelin Jr, Binding of the von Hippel-Lindau tumor suppressor protein to Elongin B and C. *Science* **269**, 1444–1446 (1995).
16. M. A. St John *et al*., Mice deficient of Lats1 develop soft-tissue sarcomas, ovarian tumours and pituitary dysfunction. *Nat. Genet.* **21**, 182–186 (1999).

17. W. Tao *et al*., Human homologue of the Drosophila melanogaster lats tumour suppressor modulates CDC2 activity. *Nat. Genet.* **21**, 177–181 (1999).
18. B. Zhao *et al*., Inactivation of YAP oncoprotein by the Hippo pathway is involved in cell contact inhibition and tissue growth control. *Genes Dev.* **21**, 2747–2761 (2007).
19. Y. Hao, A. Chun, K. Cheung, B. Rashidi, X. Yang, Tumor suppressor LATS1 is a negative regulator of oncogene YAP. *J. Biol. Chem.* **283**, 5496–5509 (2008).
20. A. Vassilev, K. J. Kaneko, H. Shu, Y. Zhao, M. L. DePamphilis, TEAD/TEF transcription factors utilize the activation domain of YAP65, a Src/Yes-associated protein localized in the cytoplasm. *Genes Dev.* **15**, 1229–1241 (2001).
21. F. Zanconato *et al*., Genome-wide association between YAP/TAZ/TEAD and AP-1 at enhancers drives oncogenic growth. *Nat. Cell Biol.* **17**, 1218–1227 (2015).
22. R. Marcotte *et al*., Functional genomic landscape of human breast cancer drivers, vulnerabilities, and resistance. *Cell* **164**, 293–309 (2016).
23. Z. Wang *et al*., Regulation of Hippo signaling and triple negative breast cancer progression by an ubiquitin ligase RNF187. *Oncogenesis* **9**, 36 (2020).
24. L. Wang, S. Zhang, X. Wang, The metabolic mechanisms of breast cancer metastasis. *Front. Oncol.* **10**, 602416 (2021).
25. R. J. DeBerardinis, N. S. Chandel, Fundamentals of cancer metabolism. *Sci. Adv.* **2**, e1600200 (2016).
26. M. E. Brunkow *et al*., Disruption of a new forkhead/winged-helix protein, scurfin, results in the fatal lymphoproliferative disorder of the scurfy mouse. *Nat. Genet.* **27**, 68–73 (2001).
27. L. Wang *et al*., Somatic single hits inactivate the X-linked tumor suppressor FOXP3 in the prostate. *Cancer Cell* **16**, 336–346 (2009).
28. M. Hisaoka, A. Tanaka, H. Hashimoto, Molecular alterations of h-warts/LATS1 tumor suppressor in human soft tissue sarcoma. *Lab. Invest.* **82**, 1427–1435 (2002).
29. S. Chakraborty *et al*., Identification of genes associated with tumorigenesis of retinoblastoma by microarray analysis. *Genomics* **90**, 344–353 (2007).
30. A. Fernandez-L, A. M. Kenney, The Hippo in the room: A new look at a key pathway in cell growth and transformation. *Cell Cycle* **9**, 2292–2299 (2010).
31. K. C. Ho *et al*., Itch E3 ubiquitin ligase regulates large tumor suppressor 1 stability. *Proc. Natl. Acad. Sci. U.S.A.* **108**, 4870–4875 (2011). Correction in: *Proc. Natl. Acad. Sci.* U.S.A. **113**, E5776 (2016).
32. B. Yeung, K. C. Ho, X. Yang, WWP1 E3 ligase targets LATS1 for ubiquitin-mediated degradation in breast cancer cells. *PLoS One* **8**, e61027 (2013).
33. Z. Salah, S. Cohen, E. Itzhaki, R. I. Aqeilan, NEDD4 E3 ligase inhibits the activity of the Hippo pathway by targeting LATS1 for degradation. *Cell Cycle* **12**, 3817–3823 (2013).
34. W. Hong, K. L. Guan, The YAP and TAZ transcription co-activators: Key downstream effectors of the mammalian Hippo pathway. *Semin. Cell Dev. Biol.* **23**, 785–793 (2012).
35. L. Yin *et al*., SH3BGRL2 inhibits growth and metastasis in clear cell renal cell carcinoma via activating hippo/TEAD1-Twist1 pathway. *EBioMedicine* **51**, 102596 (2020).
36. N. Feldker *et al*., Genome-wide cooperation of EMT transcription factor ZEB1 with YAP and AP-1 in breast cancer. *EMBO J.* **39**, e103209 (2020).
37. A. Tsherniak *et al*., Defining a cancer dependency map. *Cell* **170**, 564–576.e16 (2017).
38. Y. K. Satija, S. Das, Tyr99 phosphorylation determines the regulatory milieu of tumor suppressor p73. *Oncogene* **35**, 513–527 (2016).
39. R. Kumari, R. S. Deshmukh, S. Das, Caspase-10 inhibits ATP-citrate lyase-mediated metabolic and epigenetic reprogramming to suppress tumorigenesis. *Nat. Commun.* **10**, 4255 (2019).